HEFAT 2002
1st International Conference on Heat Transfer, Fluid Mechanics, and Thermodynamics
8 –10 April 2002, Kruger Park, South Africa
VL1

VALIDATION OF IN-TUBE CONDENSATION PERFORMANCE

Leon van der Hoek*, Leon Liebenberg, and Josua P. Meyer*****
*Master's Degree student, **Senior Lecturer, ***Professor
Department of Mechanical Engineering,
Rand Afrikaans University,
PO Box 524, Auckland Park, 2006, South Africa
E-mail: LL@ING1.RAU.AC.ZA

ABSTRACT

This paper reports on the condensation heat transfer and pressure drop performance of a heat pump water heater operating with R-22 at an average saturation temperature of 40°C with mass fluxes ranging from 300 – 800kg/m^{2}s. The purpose of the experimental work was to validate the effectiveness of a computerized data acquisition system, as well as to establish a sound experimental procedure. Experimental flow regimes were determined using a well-known flow regime predictor. This showed that the experimental data points lay mainly in the annular flow region. The experimental heat transfer coefficients and pressure drops were compared with widely used correlations, and good agreement was obtained.

INTRODUCTION

During film condensation inside tubes, various flow regimes can occur, depending on the orientation and length of the tube, heat flux along the tube axis, mass flux, and relevant fluid properties. These different flow patterns, which are dependent on mass flux, can alter heat and momentum transfers considerably, so that local calculations must be made along the length of the tube. It is therefore apparent that the prediction of the prevailing flow regime is of importance, in order to predict with confidence the heat transfer coefficient for in-tube condensation. There exist several attempts at creating *flow regime* (or *flow pattern) maps* under adiabatic conditions, as wells as flow regime maps specifically intended for condensation. Several methods have also been proposed to differentiate between stratified and non-stratified condensation. Thome (2001) is currently working on a unified flow pattern map for modelling heat transfer and pressure drop during evaporation, condensation, and adiabatic flows within horizontal, vertical, and inclined tubes.

The prediction of *pressure drop* is important when designing heat transfer systems, due to the direct relationship of pressure drop to pumping power. Furthermore, in condensers, pressure drop of the phase changing fluid may affect the mean temperature difference in the heat exchanger, and any performance evaluation should also consider this. For condensers with a small overall temperature difference, the decrease in available temperature difference due to pressure drop can have a significant effect on the heat transfer performance.

There are several empirical and analytical *heat transfer* prediction models available. The semi-empirical correlations do not include sufficient variables to accurately describe condensate flow, and the functional dependencies vary wildly. Conversely, the semi-analytical and analytical approaches usually give more accurate results than the purely empirical methods, but are cumbersome to implement practically.

This paper aims to provide validation of the performance of an R-22 operated heat pump water heater, by comparing experimental results with some of the mentioned correlations. The experimental work also serves to validate the effective operation of a computerized data acquisition system.

NOMENCLATURE

A	Surface area	m^2
AH	Area enhancement ratio (A_m/A_p)	-
Bo	Bond Number $=g(\rho_l-\rho_v)L^2/\sigma$	-
c_p	Specific heat at constant pressure	J/kgK
D	Diameter, D_i (inner); D_o (outer)	m
G	Mass velocity	kg/m^{2}s
g	Gravitational acceleration	ms^{-2}
h	Heat transfer coefficient; Specific enthalpy	W/m^{2}K; J/kg
$j_g^{\bullet}$	Dimensionless vapour mass velocity $=xG/\left[gD_i\rho_v(\rho_l-\rho_v)\right]^{0.5}$	
k	Thermal conductivity	W/mK
L	Effective heat exchanger length	m
$\dot{m}$	Mass flow-rate	kg. s^{-1}
p	Pressure	Pa
Pr	Prandtl number $(=\mu c_p/k)$	-
$\dot{Q}$	Heat rate	W
Re	Reynolds number $(=GD/\mu)$	-
T	Temperature, T_w (water); T_{sat} (saturation)	°C

U	Overall heat transfer coefficient	W/m^2K
x	Vapour quality	-
X_{tt}	Lockhart-Martinelli parameter for turbulent-turbulent flow $=\left[(1-x)/x\right]^{0.9}\left(\rho_g/\rho_l\right)^{0.5}\left(\mu_l/\mu_g\right)^{0.1}$	-
z	Distance traveled by water	m

Greek letters

μ	Dynamic viscosity	Ns/m^2
ρ	Density	kg/m^3
Δ	Difference	-
Δp	Pressure drop	**kPa**

Subscripts

ave	average	Cu	copper tube
i	inside, inlet	*l*	liquid phase
o	outside, outlet	v	vapour phase

EXPERIMENTAL FACILITY

The vapour compression loop

The main system components were a reciprocating compressor (9.6kW at 10°C evaporating and 45°C condensing temperature) with suction accumulator, water-cooled condenser, a manually adjustable expansion valve, and a water-heated evaporator, as shown in Fig. 1.

The test condenser consisted of eight (8) coaxial tube condenser sections connected in series, each section (labelled A through H in Figure 1) having an effective heat transfer length of 1.5m. The distance between pressure drop measuring points was 1.4m. The inner tube of each condenser had an outside diameter of 9.52mm (3/8in), whilst the outer tube had an outside diameter of 19.05mm (3/4in). Cooling water flowed in the annulus and refrigerant in the inner tube in a counter-flow direction. Refrigerant mass flow rate through the condensers was controlled by means of a refrigerant bypass line, which was connected in parallel with the test condenser. A water-cooled after-condenser (7kW capacity) was used to ensure that only liquid refrigerant entered the Coriolis-type mass flow meter. Sight glasses before and after the refrigerant Coriolis flow meter were used to verify that only liquid (i.e. sub-cooled) refrigerant flowed through it. All test sections were thermally insulated with foam rubber.

Temperatures were measured with resistance temperature detectors (RTDs) at all the refrigerant and water inlets and outlets, for both the condenser and evaporator. At each of the measurement locations, two RTDs were positioned, one at each side of the outer tube.

The absolute pressures of the condensing refrigerant were measured with a large-dial pressure gauge, as well as strain-gauge type pressure transducers situated at the inlet and outlet of each of the condenser sub-sections.

The water loops

Two main water loops were used, one flowing through the condensing side (i.e. the chilled water loop) and the other through the evaporating side (i.e. the hot water loop).

On the condensing side the water temperature was kept constant in a 1 000 litre capacity insulated reservoir connected to a 15 kW chiller. A positive displacement pump pumped the chilled water to the double-tube condenser. The flow rate of the water through the test sections was measured with a Coriolis mass flow meter. After passing through the condenser, the water returned to the reservoir of the chiller unit.

A similar flow loop was used on the evaporating side, also with an insulated 1 000-litre reservoir, but connected to a 12 kW electric resistance heater. Increasing or decreasing the temperature of the water through the evaporator altered the refrigerant density at the compressor inlet and thus the refrigerant mass flow.

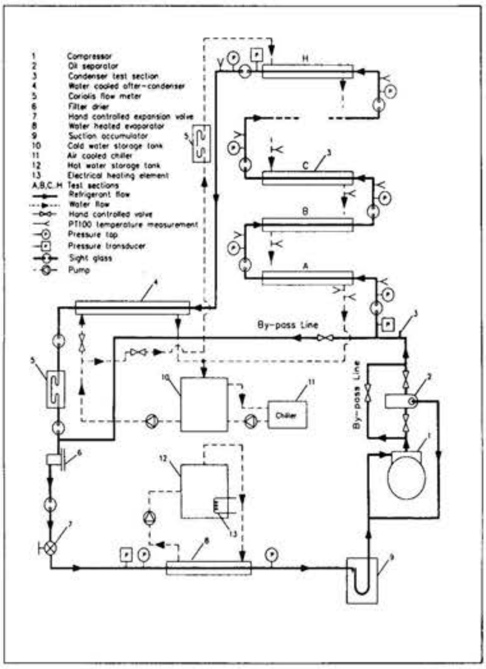

Fig. 1: Experimental set-up

Experimental uncertainties

The experimental uncertainties for the different quantities were estimated with a propagation-of-error analysis (Kline and McClintock 1953). Table 1 shows the predicted uncertainties.

Table 1: Instrumentation ranges and uncertainty

Quantity	*Uncertainty*
Absolute temperature	± 0.17°C
Differential temperature	± 0.08°C
Absolute pressure	±0.15% p_{max}
Differential pressure	±0.05% p_{max}
Mass flow rate: water, refrigerant	$\dot{m}$ < 0.03kg/s: ± 0.5% $\dot{m}$ ± 0.044% $\dot{m}$ > 0.09kg/s: ± 0.1% $\dot{m}$ ± 0.044%
Vapour quality	±0.05%
Heat transfer coefficient	±15% at low mass fluxes; ±8% at high mass fluxes

Experimental ranges

Table 2 shows the ranges of experimental parameters covered.

Table 2: Ranges of experimental quantities covered

Experimental quantity	*Range covered*
Refrigerant mass flux, kg/(m²s)	300, 400, ..., 800
Overall Condensing Heat Transfer Coefficient, W/(m².°C)	343 – 2 716
Vapour quality (total, nominal), -	0.05 – 0.9
Condensation temperature (nominal), °C	40

Data acquisition

Data were gathered by a computerized data acquisition system. The LabVIEW® program (NIST 2000) displayed all measured quantities in real time. In addition, secondary quantities such as refrigerant quality, heat transfer coefficient and various dimensionless groups were output to the screen. This allowed the user to closely monitor system parameters until they reached target values.

DATA REDUCTION

Annulus-side heat transfer coefficient (for single-phase flow)

A modified Wilson Plot technique (Briggs and Young 1969) was used to determine the unknown Reynolds number exponent and annulus-side coefficient for the heat transfer coefficient:

$$h_o = 0.0936\frac{k_{l,o}}{D_i}\mathrm{Re}_{l,o}^{0.742}\,\mathrm{Pr}_{l,i}^{1/3}\left(\mu_l/\mu_{l,w}\right)_o^{0.14} \qquad (1)$$

Deduction of average heat transfer coefficient

The average refrigerant-side heat transfer coefficient was calculated from:

$$h_i = \frac{1}{A_i}\left[\frac{1}{UA} - \frac{1}{h_o A_o} - \frac{\ell n\left(D_o/D_i\right)}{2\pi k_{Cu} L}\right]^{-1} \qquad (2)$$

where h_o is the waterside heat transfer coefficient determined from the Modified Wilson plot procedure.

Deduction of semi-local heat transfer coefficient

The semi-local heat transfer coefficient for the refrigerant-side was determined from:

$$h_i = \frac{1}{\dfrac{(T_r - T_w)\pi D_i}{\dot{m}c_{p,w}\dfrac{dT_w}{dz}} - \dfrac{D_i}{h_o A_o} - \dfrac{D_i \cdot \ell n\left(D_o/D_i\right)}{2k_{Cu}}} \qquad (3)$$

Deduction of Vapour Quality

The average sectional vapour quality was calculated from:

$$x_{ts,i} = \frac{h_{ts,i} - h_l}{h_l - h_v} \text{ with } h_l \text{ and } h_v \text{ measured at } T_{ts,i}$$
$$x_{ts,o} = \frac{h_{ts,o} - h_l}{h_l - h_v} \text{ with } h_l \text{ and } h_v \text{ measured at } T_{ts,o} \qquad (4)$$

The average vapour quality of each test sub-section was then used:

$$x = \frac{x_{ts,i} + x_{ts,o}}{2} \qquad (5)$$

Pressure Drop (average and semi-local)

The *average* pressure drops were obtained by plotting the variation of pressure drop with mass flux. The pressure drops were measured with an approximate inlet quality of 90% and an outlet quality of 10%.

The *semi-local* pressure drops were calculated by plotting the pressure drops per unit length (i.e. the pressure gradients) versus the average vapour quality.

EXPERIMENTAL RESULTS

Flow regimes

Figure 2 shows the experimental Breber et al. (1980) map for the experimental work conducted. The majority of data points fall in the annular flow regime. As the mass flux increases, the experimental points move from the slug/plug flow region, and the transitional regions, to the annular/mist (spray) areas, implying that forced convection becomes the main driving mechanism of heat transfer.

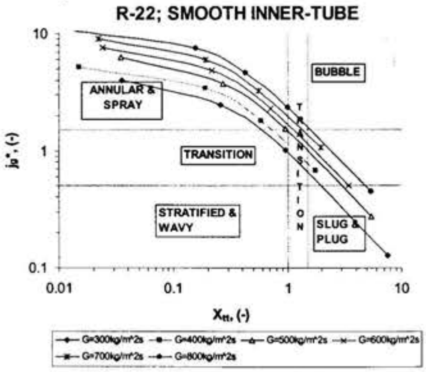

Fig. 2: Breber et al. (1980) map for experimental data

At the lowest mass flux of 300kg/m²s, two different flow regimes were observed as the vapour quality was changed. Transitional wavy flow occurred at low qualities, followed by annular flow for medium and high quality values. At the high mass fluxes of 500, 600, 700 and 800kg/m²s, the flow regimes included transitional wavy flow at qualities below approximately 0.15, and annular flow for approximately $0.15 < x < 0.3$, and mist flow for approximately $x > 0.3$. It is apparent that at high mass fluxes, the predominant flow patterns are annular and annular-mist (viz. in greater than 70% of the condensation path).

Semi-local and average heat transfer coefficients

Figures 3 and 4 present the semi-local heat transfer data. At low mass flux, the heat transfer coefficient increases modestly with quality. As mass flux increases, and especially at vapour qualities above 30%, the heat transfer coefficient displays a much more pronounced effect of quality. At high mass fluxes, even at low vapour qualities, the heat transfer coefficients were substantially higher than those for the low mass flux cases.

Furthermore, a high vapour quality (i.e. large void fraction) results in a greater mixture velocity than at low quality, due to vapour having a much larger specific volume than liquid). Heat transfer coefficient is dependent on flow velocity, hence larger heat transfer coefficients are expected for higher quality flows.

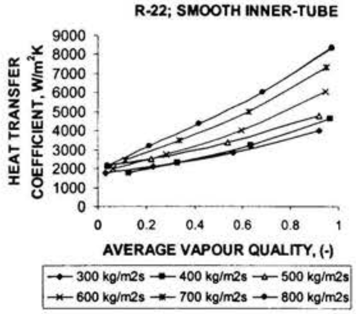

Fig. 3: Variation of the semi-local heat transfer coefficient at various mass fluxes

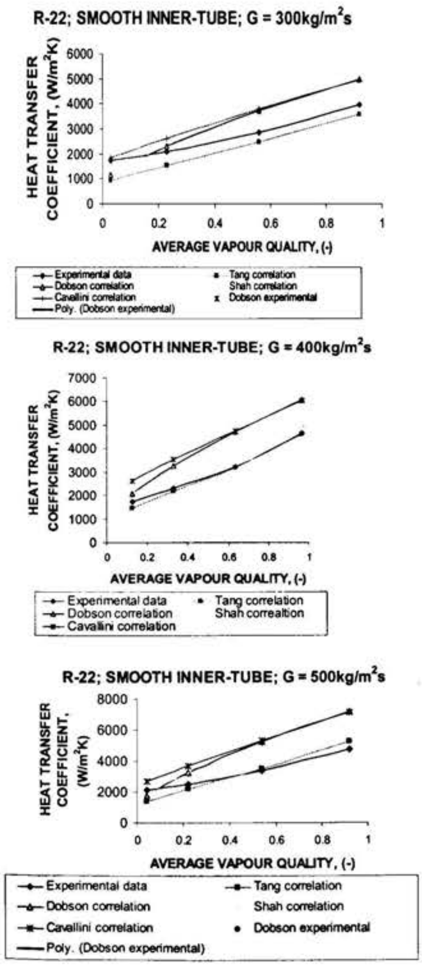

Fig. 4: Semi-local heat transfer coefficients at various mass fluxes (continues)

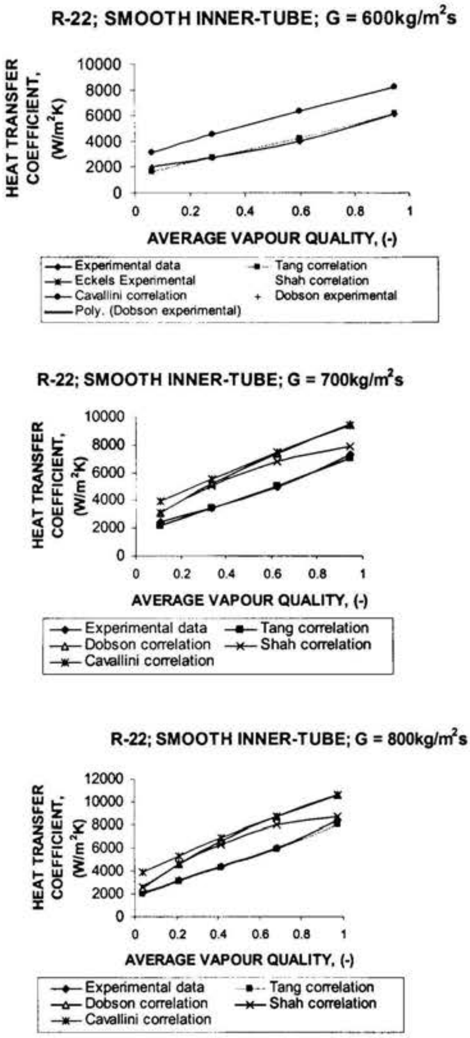

Fig. 4: Semi-local heat transfer coefficients at various mass fluxes

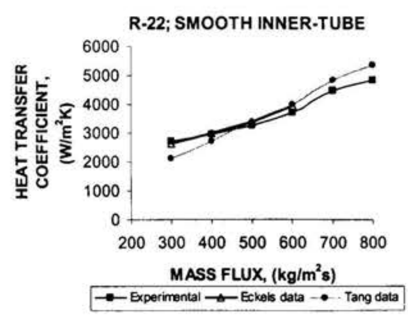

Fig. 5: Average heat transfer coefficients for condensing R-22 at 40°C saturation temperature

Comparison with heat transfer correlations

Due to the fact that more than 70% of the data points lie in the annular flow regime, only such heat transfer and pressure drop correlations were used in the comparative studies (c.f. Figures 3, 4, and 5). The chosen annular flow correlations for purpose of comparison are those of Cavallini and Zecchin (1974), Shah (1979), Tang (1997), Dobson et al. (1998), and the experimental data of Eckels and Tesene (1999 a).

The authors' experimental data agrees to within −12% (mean deviation) of the Tang correlation, whilst all the other correlations over predict the data (Cavallini and Zecchin: 42%; Shah: 21%; Dobson et al.: 33%).

Semi-local and average pressure drops

The average experimental pressure drops are shown in Fig. 6. It is apparent that the average experimental pressure drop increases with increase in mass flux.

The experimental average pressure drop data were compared with a number of currently available pressure drop correlations. Correlations for the frictional component of the pressure drop were obtained from Lockhart and Martinelli (1949), Dukler et al. (1964), and Souza et al. (1992). The void fraction models of the following researchers were used in conjunction with the mentioned pressure drop correlations: Zivi (1964), Rouhani and Axelsson (1970), and Graham et al. (1999). It is apparent from Fig. 6 that the average experimental pressure drop increases with increase in mass flux.

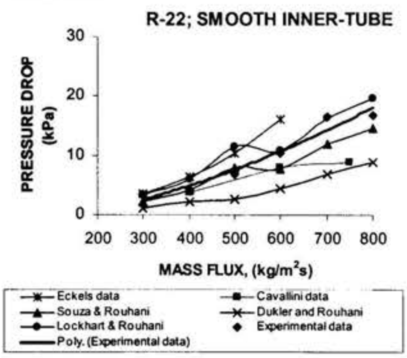

Fig. 6: Average condensation pressure drop

Figure 7 shows the pressure drop per unit length (i.e. the "semi-local" pressure drop) for R-22 as a function of average vapour quality. Figure 7 also shows that the pressure gradient increases significantly with refrigerant vapour quality. For constant mass fluxes, the pressure drop also increases with increasing vapour quality for most of the vapour quality range. The exception to this trend is at higher qualities, where the pressure drop decreases as the vapour quality increases. As the vapour quality increases, the vapour speed becomes even higher, producing greater pressure drops. But increasing the vapour quality also reduces the thickness of the liquid annulus (Liebenberg et al. 2000). At high vapour qualities, therefore, the liquid annulus becomes very thin and eventually disappears at extremely high qualities, causing a reduction in pressure drop.

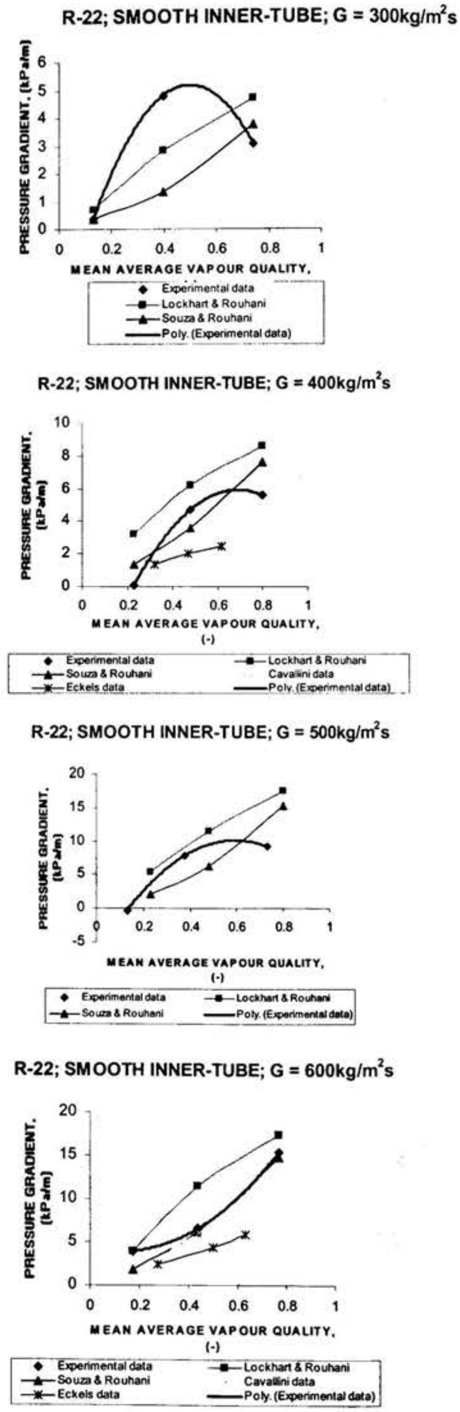

Fig. 7: Pressure drop per unit length as a function of average quality (continues on next page)

R-22; SMOOTH INNER-TUBE; G = 700kg/m²s

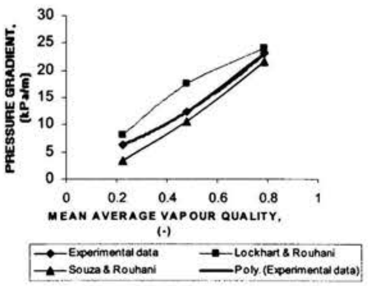

R-22; SMOOTH INNER-TUBE; G = 800kg/m²s

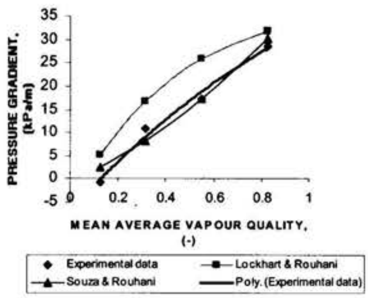

Fig. 7: Pressure drop per unit length for R-22 shown as a function of average quality

Comparison with pressure drop correlations

The experimental data are predicted within −14% by the Souza et al. (1992)/Rouhani and Axelsson (1970) correlation. The Dukler et al. (1964) correlation under-predicts by an average of −55%, whilst the Lockhart and Martinelli (1948) correlation under-predicted the data by an average of 22%. The choice of void fraction model did not make much of a difference with the latter two correlations.

CONCLUSIONS

Heat transfer coefficients and pressure drops were determined for a heat pump water heater operating with R-22. Good agreement was obtained with widely used correlations, thus validating the effectiveness of the computerized data acquisition program, the experimental procedure, and in the soundness of the experimental heat pump facility.

REFERENCES

Briggs, D.E. and Young, E.H., 1969, "Modified Wilson Plot Techniques for Obtaining Heat Transfer Correlation for Shell and Tube Heat Exchangers," *Chem. Eng. Prog. Symp.*, Serial, 92, Vol. 65, pp. 34-45.

Cavallini, A. and Zecchin, R., 1974, "A Dimensionless Correlation for Heat Transfer in Forced Convection Condensation," *Proc. Vth. Int. Heat Transfer Conference, JSME,* Vol. 3, pp. 309-313.

Dobson, M.K., 1994, Ph.D thesis: "Heat Transfer and Flow regimes during Condensation in Horizontal Tubes," Graduate College of the University of Illinois at Urbana-Champaign, Urbana, Illinois, USA.

Dobson, M.K. and Chato, J.C., 1998, "Condensation in Smooth Horizontal Tubes," *ASME Journal of Heat Transfer,* Vol. 120, pp. 193-213.

Dukler, A.E., Wicks, M., and Cleveland, R.G., 1964, "Frictional Pressure Drop in Two-Phase Flow," *AIChE Journal*, Vol. 10, pp. 44-51.

Eckels, S.J., and Tesene, B.A., 1999 a, "A Comparison of R-22, R-134a, R-410A, and R-407C Condensation Performance in Smooth and Enhanced Tubes, Part I: Heat Transfer," *ASHRAE Transactions,* Vol. 105, pp. 428 – 441.

Eckels, S.J., and Tesene, B.A., 1999 b, "A Comparison of R-22, R-134a, R-410A, and R-407C Condensation Performance in Smooth and Enhanced Tubes, Part II: Pressure Drop," *ASHRAE Transactions,* Vol. 105, pp. 442 –452.

Graham, D.M., Kopke, H.R., Wilson, M.J., Yashar, D.A., Chato, J.C., and Newell, T.A., 1999, "An Investigation of Void Fraction in the Annular/Stratified Flow Regions in Smooth, Horizontal Tubes,"*ACRC TR-144, Air Conditioning and Refrigeration Center,* University of Illinois at Urbana-Champaign.

Kline, S.J., and Mc Clintock, F.A., 1953 "Describing Uncertainties in Single-Sample Experiments," *Mechanical Engineering,* Vol. 75, pp. 3 – 8.

Liebenberg, L., Bergles, A.E., and Meyer, J.P., 2000, A Review of Refrigerant Condensation in Horizontal Micro-Fin Tubes," *AES Vol. 40, Proceedings of the ASME Advanced Energy Systems Division,* pp. 155 – 168.

Lockhart, R.W. and Martinelli, R.C., 1949, "Proposed Correlation of Data for Isothermal Two-phase, Two-component Flow in Pipes," *Chemical Engineering Progress,* Vol. 45, No. 1, pp. 39-48.

NIST, 2000, *LabVIEW Programming Manual,* National Instruments, Inc., Austin, TX, USA.

Rouhani, Z. and Axelsson, E. (1970). Calculation of volume void fraction in the subcooled and quality region, *Int. J. Heat Mass Transfer*, Vol. 13, pp. 383-393.

Souza, A.M., Chato, J.C., Jabardo, J.M.S., Wattelet, J.P., Panek, J., Christofferson, B., and Rhines, N., 1992, "Pressure Drop During Two-Phase Flow of Refrigerants in Horizontal Smooth Tubes," ACRC TR-25, Air Conditioning and Refrigeration Center, University of Illinois at Urbana-Champaign, October.

Souza, A.L., Pimenta, M.M., 1995, "Prediction of Pressure Drop during Horizontal Two-Phase Flow of Pure and Mixed Refrigerants," *ASME Conference on Cavitation and Multiphase Flow,* FED-Vol. 210, pp. 161 – 171.

Tang, L., 1997, "Empirical Study of New Refrigerant Flow Condensation inside Horizontal Smooth and Micro-fin Tubes," *Ph.D. thesis,* University of Maryland at College Park.

Thome, J.R., 2001, *Personal communication.* Professor, Faculty of Engineering Science, Laboratory of Heat and Mass Transfer, Swiss Federal Institute of Technology, Lausanne, Switzerland.

Zivi, S.M., 1964, "Estimation of Steady State Steam Void-Fraction by means of Principle of Minimum Entropy Production," *Trans. ASME, Series C,* Vol. 86, pp. 237-252.